Photorefractivity in poly(N-vinylcarbazole)-based polymer composites

Malliaras, George G.; Krasnikov, Victor V.; Bolink, Henk J.; Hadziioannou, Georges

Published in:
Pure and Applied Optics

DOI:
10.1088/0963-9659/5/5/017

Publication date:
1996

Pure Appl. Opt. **5** (1996) 631–643. Printed in the UK

Photorefractivity in poly(*N*-vinylcarbazole)-based polymer composites

George G Malliaras†, Victor V Krasnikov, Henk J Bolink and Georges Hadziioannou

Polymer Chemistry Department, Materials Science Centre, University of Groningen, Nijenborgh 4, 9747 AG, Groningen, The Netherlands

Abstract. The mechanism of photorefractivity in a family of model composites based on PVK is discussed. Novel aspects of photorefractivity that are unique in polymers are described. The effect of plasticization on their photorefractive performance is investigated.

1. Introduction

The photorefractive effect is observed in materials that are both electro-optic and photoconducting. If such a material is illuminated with a nonuniform light intensity pattern, charge generation takes place at the bright areas. These photogenerated charges migrate and eventually get trapped at the dark areas, a process which can take place through several cycles of photogeneration, diffusion and/or drift and trapping. The resulting charge redistribution creates an internal electric field, the space charge field E_{SC}, which changes the refractive index via electro-optic effects. In this way, light intensity patterns are replicated into refractive index gratings, with obvious potential applications in optical data storage and processing [1].

Compared to other mechanisms that lead to photoinduced changes of the optical properties (such as photochromism, thermorefraction, etc), the photorefractive effect possesses a combination of characteristics which make it very attractive for applications: very high refractive index changes can be achieved even with weak laser beams, as a result of the integrating nature of the effect. The resulting refractive index gratings are reversible, as uniform illumination erases the space charge field. Another very important characteristic is the existence of a spatial phase shift between the illumination pattern and the refractive index grating, which is the genuine signature of the photorefractive effect: no other mechanism can produce a phase-shifted refractive index grating. The existence of this phase shift gives rise to steady state asymmetric energy exchange between two laser beams, which is the basis for several specific applications [1].

Until a few years ago, the photorefractive effect was only observed in certain inorganic electro-optic crystals. The observation of the effect in a polymer, in 1991 [2], created an alternative, very promising class of photorefractive materials. Processability is one of their main advantages, while tunability is inherent in the way they are fabricated. Moreover, potentially better performance is foreseen, as a result of the different mechanism of the refractive index change [3].

† E-mail address: georgem@rugch5.chem.rug.nl

0963-9659/96/050631+13$19.50

The field of polymer photorefractivity has strongly benefitted from earlier studies of the optoelectronic properties of polymers. The required functionalities of photoconductivity and the electro-optic effect are given to a polymer with the addition of specific functional molecules or monomers, that can be placed in three different positions: incorporated on the polymer backbone, attached as a pendant side group or simply doped into the polymer. On the basis of this, photorefractive polymers are classified into two main groups: fully functionalized, where all the components are attached onto the polymer backbone and composites, where low molecular weight dopants are present.

The processes of charge generation and transport are rather well studied in polymers due to their application in xerography [4]. Hole transport with a relatively high drift mobility can be achieved with doping or chemically attaching donor-like species (from now on referred to as charge transport species) on an inert polymer backbone. With the addition of proper sensitizers, a high quantum yield of charge generation in the visible is achieved. The electro-optic functionality is provided in the polymer by adding dipolar molecules with a large hyperpolarizability (from now on referred to as nonlinear optical (NLO) molecules) and partially aligning them by poling close to the glass transition temperature (T_g) [5]. In the case of composites where the T_g is low enough, poling can be achieved *in situ*, at room temperature.

In figure 1, a schematic representation of the space charge field formation process in a photorefractive polymer is shown. Indicated are the highest occupied and the lowest unoccupied molecular orbitals (HOMO and LUMO, respectively) of the inert polymer backbone, the sensitizer (charge generating (CG) site) and the NLO molecule, together with the HOMOs of the charge transport (CT) and trapping (TS) sites. In this picture, photoionization of the charge transfer complex between the sensitizer and the charge transport species is depicted and a hole is transferred to a charge transport site from where it migrates via hopping until it gets trapped at a low ionization potential site. In this picture,

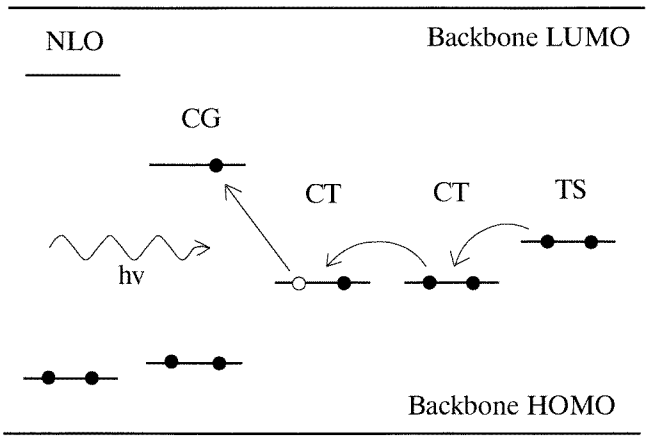

Figure 1. A schematic representation of the space charge field formation process in a photorefractive polymer. Indicated are the highest occupied and the lowest unoccupied molecular orbitals (HOMO and LUMO, respectively) of the inert polymer backbone, the sensitizer (charge generating (CG) site) and the NLO molecule, together with the HOMOs of the charge transport (CT) and trapping (TS) sites. LUMOs of the latter are not shown for clarity. A hole which is created by photoionization of the charge transfer complex between the sensitizer and the charge transport species, migrates through hopping among charge transport species, until it gets immobilized at a site of a trap.

the NLO molecule does not contribute to the space charge field formation process. Although it can act as a sensitizer at shorter wavelengths, it is preferable to have the functionalities of charge generation and the electro-optic effect well separated [6].

The first unambiguous observation of the photorefractive effect in a polymer was in an electro-optic epoxy doped with the charge transport molecule 4-(*N*,*N*-diethylamino)benzaldehyde diphenylhydrazone (DEH) [2]. The diffraction efficiency was 2×10^{-5} and the typical response time several minutes. Soon, photorefractivity was reported in several other composites, as well as fully functionalized materials [7]. The observation of net gain in a poly(*N*-vinylcarbazole) (PVK) based polymer doped with an NLO molecule [8] marked the beginning of a new era in polymer photorefractivity. The superior performance of this material was found to arise from the existence of an enhancement mechanism, which relies on the ability of the NLO molecules to reorient under the influence of the space charge field [3]. With efficient plasticization, this enhancement can be optimized and, as a result, several similar composites with diffraction efficiency approaching 100% were prepared [9–12].

In this paper, the mechanism of photorefractivity in a family of model composites based on PVK is discussed. For the preparation of these composites, PVK is sensitized with 2,4,7-trinitro-9-fluorenone (TNF) or C_{60} and doped with the NLO molecules 4-(diethylamino)nitrobenzene (EPNA) or 4-(hexyloxy)nitrobenzene (HONB). This paper is organized as follows: in section 2, a brief description of the sample preparation and of the measurement procedures is given. In section 3, some novel aspects of photorefractivity that are unique to polymers are discussed. First, the origin of the refractive index change is shown to be different from that in crystalline photorefractive materials. Second, a modification of the trap density of the composites is demonstrated with the addition of DEH. Third, the space charge field formation process is shown to depart from its expected behaviour, due to the presence of disorder. Finally, in section 4, the effect of addition in the composite of *N*-ethylcarbazole (ECZ), which acts as a plasticizer, is investigated. The properties of the photorefractive gratings in the plasticized composites are discussed and a geometry of interaction that results in enhanced performance is described.

2. Experiment

Secondary standard PVK was purchased from Aldrich and was precipitated three times from chloroform in diethylether. ECZ was purchased from Aldrich and recrystallized twice from ethanol. TNF was purchased and dried under vacuum over P_2O_5 for two days. EPNA was synthesized by aromatic substitution of 4-fluoronitrobenzene with diethylamine and recrystallized from a mixture of dichloromethane and pentane (1:4). HONB was synthesized by a substitution reaction between 4-nitrophenol and 6-bromohexane and recrystallized from a mixture of dichloromethane and pentane (1:4). DEH was prepared by condensation of 4-(diethylamino)benzaldehyde with 1,1-diphenylhydrazine and recrystallized twice from a mixture of dichloromethane and pentane (1:1). The chemical structures of these compounds are shown in figure 2.

For the preparation of the samples, proper amounts of the compounds were dissolved in spectroscopic grade chloroform. The solution was filtered, the solvent was extracted and the solid deposit was reduced into powder that stayed overnight in a vacuum chamber (pressure lower than 10^{-2} Torr) to ensure maximum solvent removal. Subsequently, thick pellets were prepared, that were sandwiched between two ITO covered glass plates by heating above the glass transition temperature. Teflon spacers were used to fix the film thickness to 100 μm.

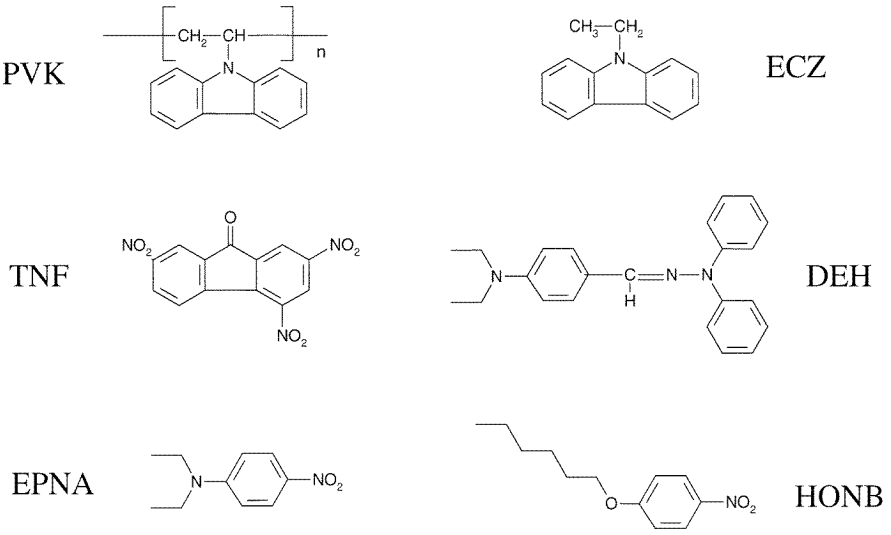

Figure 2. Chemical structures of the compounds.

The electro-optic coefficient of the samples was evaluated with the ellipsometric technique described by Schildkraut [13]. For the holographic studies of photorefractivity in polymers, the tilted geometry was used, with the two beams from a He–Ne laser incident on the sample at external angles 30° and 60°, unless otherwise stated. The grating spacing in this configuration was approximately 1.6 μm. The diffraction efficiency was measured in a backward degenerate four-wave mixing (DFWM) arrangement. The grating was written using two s-polarized beams with the same power, equal to approximately 600 mW cm^{-2} outside the sample and the diffraction efficiency was measured using a weaker, p-polarized beam from a separate He–Ne laser. The phase shift of the photorefractive grating was measured with the two-beam coupling (2BC) method [14, 15], using two p-polarized writing beams. The gain coefficient was evaluated by measuring the energy exchange between the two writing beams. Experimental details can be found in [16].

3. Novel aspects of photorefractivity in polymers

PVK is a promising material for photorefractive applications. It can be processed into good optical quality films, which absorb in the ultraviolet region of the spectrum. With the addition of small amounts of a sensitizer like TNF or C_{60}, it exhibits photoconductivity throughout the visible [4]. EPNA and HONB were selected as NLO molecules because of their extended transparency in the visible, which makes it less likely that they interfere with the space charge field formation process. In this section, some novel aspects of photorefractivity that are unique in polymers are discussed on composites that contain 40% wt EPNA or HONB and 0.1% wt TNF relative to PVK.

3.1. The origin of the refractive index change

In crystalline photorefractive materials, the space charge field (E_{SC}) changes the refractive index via the linear (Pockels) electro-optic effect:

$$\Delta n = -\tfrac{1}{2} n_0^3 r_{\text{eff}} E_{SC} \tag{1}$$

where r_{eff} is the linear electro-optic coefficient and n_0 the refractive index. However, in host–guest polymers like the composites discussed here, other effects may also be present [17]: as no physical linkage exists between the NLO molecules and the polymer backbone, relatively little constraint is present to prohibit their orientational mobility [18]. During photorefractive grating growth, the NLO molecules are under the influence not only of the external field, but also of the space charge field, which can be of a comparable magnitude. It is thus expected that their orientation will be modulated by the space charge field, causing a spatial variation of the birefringence and the electro-optic coefficient. Both these effects can contribute to the total refractive index change, leading to an increase of the diffraction efficiency; a mechanism known as the orientational enhancement of photorefractivity [3].

The presence of the orientational enhancement can be checked by polarization anisotropy (the ratio between the change in refractive index for p- and for s-polarized light, Δn_p and Δn_s, respectively) measurements. In the case of a pure linear electro-optic effect, the ratio $\Delta n_p/\Delta n_s$ is solely determined by the ratio r_{33}/r_{13} (which is equal to 3 for poled polymers [5]) and is always positive. This is clearly not the case in figure 3, where the modulation of the intensity of one of the beams during a two-beam coupling experiment is shown for p- and s-polarized light. The modulation of the transmitted intensity I is given by [14]

$$I \propto \Delta n \sin(\varphi + 2\pi v t/\Lambda_G) \tag{2}$$

where φ is the phase shift of the photorefractive grating, v is the velocity of the sample translation and Λ_G is the grating spacing. The negative $\Delta n_p/\Delta n_s$ that is revealed in figure 3, shows that the orientational enhancement mechanism is operational in the PVK:TNF:EPNA composite [10, 19].

3.2. Control of charge trapping

In contrast to the process of charge generation and transport, charge trapping in polymers remains a vaguely understood process. Identification of the trapping sites is still a subject of investigation even in the case of well studied inorganic photorefractive crystals. Apart from its fundamental importance, understanding and optimization of the charge trapping process is very important for the tuning of the performance of photorefractive materials. The space charge field depends strongly on the saturation field, which is proportional to the trap density. The response time of the photorefractive effect is also dependent on the presence of traps.

According to the scheme of figure 1, trapping is expected to take place at sites with ionization potential lower than that of the transport species. Thus, by introducing a low ionization potential molecule such as DEH, a modification of the trap density of the photorefractive composite should occur. This is shown in figure 4, where the inverse response time τ^{-1} under uniform illumination (600 mW cm^{-2}) is plotted for samples with various amounts of DEH (here τ refers to the response time of the space charge field). A sharp decrease of τ^{-1} is observed for the samples with small amounts of DEH, in agreement with an increased trap density. Using a molecule with even lower ionization potential instead of DEH, a longer decrease of the response time should be possible.

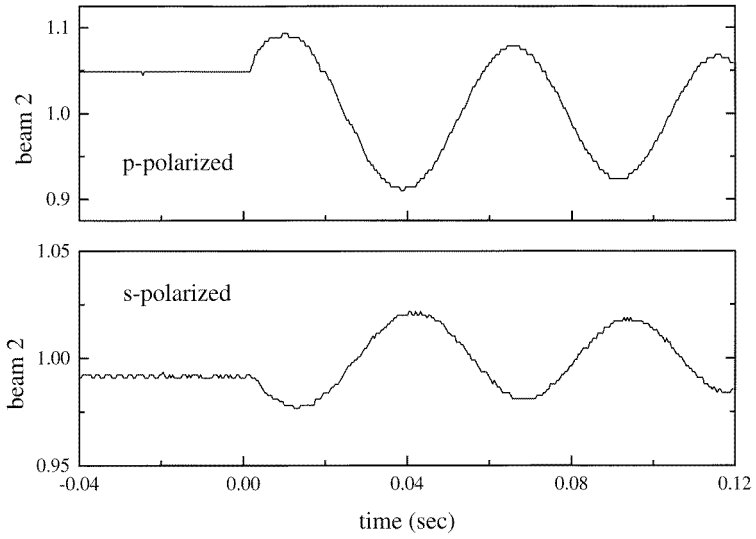

Figure 3. Two beam coupling traces from the PVK:TNF:EPNA composite, for p- and for s-polarized light. Only the second beam is shown in both cases.

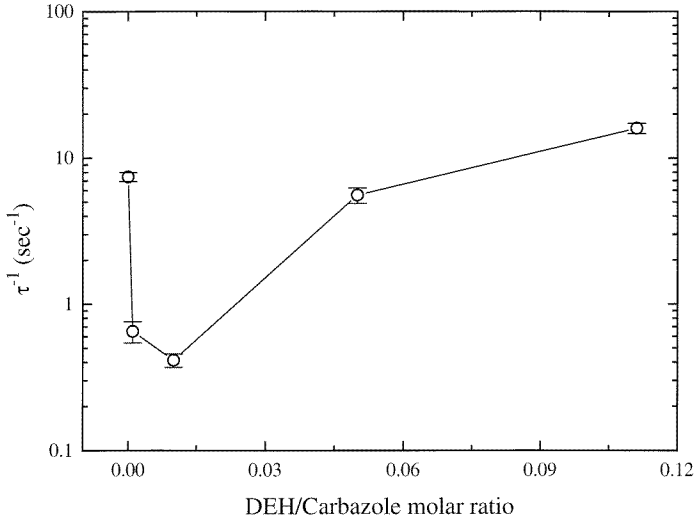

Figure 4. Inverse response time of the photorefractive grating as a function of the DEH/carbazole molar ratio, at the same electric field. The line is a guide for the eye.

The recovery of τ^{-1} for the samples with higher DEH concentration is due to the establishment of a new transport channel—in this regime, the DEH molecules are close enough so that direct hopping of charge from one DEH molecule to another is possible. The variation of the phase shift of the refractive index grating [20] and of the hole drift mobility [21] corroborate this picture. From the above it is clear that there is an optimum value for the concentration of the trapping species, in order to achieve the maximum trap density.

3.3. The influence of disorder

Much of our understanding of the photorefractive effect relies on knowledge gathered from investigations of inorganic crystals, as described by the standard model of photorefractivity [22]. Although the picture of the space charge field formation in polymers is similar, the nature of charge transport in this class of materials is very distinct—charge transport in polymers takes place via hopping. Due to the presence of positional and energetic disorder among the hopping sites, charge packets exhibit anomalous propagation characteristics and the drift mobility is strongly electric field and temperature dependent [23]. This can be measured with a holographic time-of-flight (HTOF) experiment.

In HTOF, an interference pattern from two pico- or nanosecond laser pulses creates a sinusoidal distribution of mobile carriers, which drifts under the influence of an external electric field. As charge separation advances, a space charge field builds up that can be probed with a CW laser beam through the electro-optic effect. One measures the diffraction efficiency $\eta(t)$ [24]

$$\eta(t) \propto (r_{\text{eff}} E_{\text{SC}}(t))^2 \tag{3}$$

where r_{eff} is the effective electro-optic coefficient and $E_{\text{SC}}(t)$ is the space charge field. As the mobile carriers drift relative to the immobile distribution of the countercharges, the space charge field shows an oscillatory behaviour, that is reflected in the temporal behaviour of the diffraction efficiency [24, 25]. Transient holographic experiments of this kind are used to provide valuable information related to the charge transport process and to determine the carrier drift mobility [25, 26].

In the case of polymers, however, the space charge field shows a different temporal behaviour; as can be seen in figure 5, the diffraction efficiency increases to a maximum and then slowly decays to a plateau value, without showing any oscillation. This was found to be an inherent property of the samples, independent of the grating spacing [27]. This behaviour of the diffraction efficiency reflects the influence of disorder on the space charge field formation process: the HTOF trace in the inset of figure 5, which looks identical to

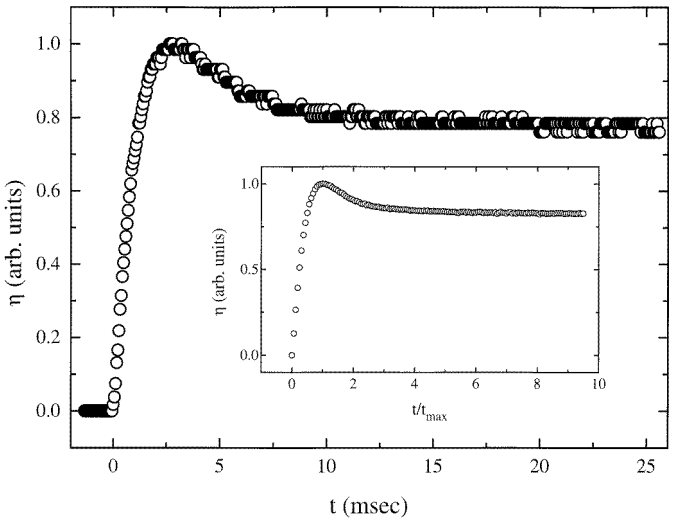

Figure 5. Typical HTOF trace in PVK:TNF:HONB, at room temperature. Inset: a computer simulation of the HTOF trace.

the experimental one, is a result of a computer simulation [28] based on the theory of Scher and Montroll for charge transport in disordered materials [29].

4. Placticization of the composites

As the orientational mobility of the NLO molecules is higher in the neighbourhood of the glass transition temperature, the effective electro-optic coefficient (including the contribution from Kerr effects) is maximized if the T_g of the composite is close to room temperature. The T_g of pure PVK is around 200 °C. With the addition of 40% wt of EPNA it is lowered to approximately 120 °C [16]. Therefore substantial room exists for improvement with the incorporation of additional plasticizer.

4.1. Influence of the concentration of plasticizer

In figure 6, the electro-optic coefficient, the gain coefficient and the square root of the diffraction efficiency are shown for composites containing 30% wt EPNA, 0.1% wt C_{60} and a variable amount of ECZ (all relative to the total film weight). The increase of the electro-optic coefficient with ECZ concentration comes as a result of the enhanced orientational mobility of EPNA, due to a lowering of the T_g. DSC measurements support this conclusion. However, we were unable to measure the exact value of the T_g of the plasticized samples, due to the broad nature of the transition.

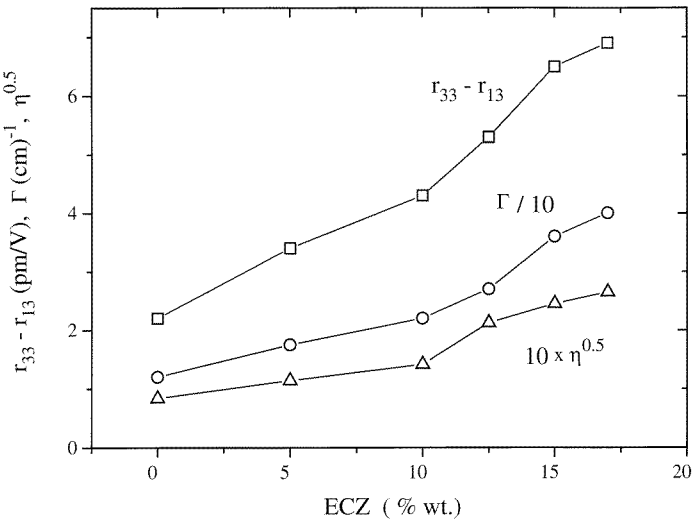

Figure 6. The variation of the electro-optic coefficient (at 20 V μm^{-1} and 1 kHz), the gain coefficient divided by ten (at 55 V μm^{-1}) and the square root of the diffraction efficiency multiplied by ten (at 55 V μm^{-1}) as a function of the ECZ concentration.

The gain coefficient Γ depends linearly on the effective electro-optic coefficient [22]

$$\Gamma \approx r_{\mathrm{eff}} E_{\mathrm{SC}} \sin\varphi \tag{4}$$

and the same holds for the square root of the diffraction efficiency η [22]

$$\eta^{0.5} \approx r_{\mathrm{eff}} E_{\mathrm{SC}} . \tag{5}$$

The dependence of Γ and $\eta^{0.5}$ on the ECZ concentration is similar to that of the electro-optic coefficient, indicating that the enhanced performance comes only as a result of the higher orientational mobility of the NLO molecules and that the plasticizer does not affect the magnitude of the space charge field.

Further increase of the ECZ concentration resulted in a higher electro-optic response. However, the composites with concentration higher than 20% wt suffered from electric-field-induced crystallization of EPNA. This crystallization occurred mainly near the polymer–ITO interfaces. For this reason, further investigation was carried out using the composite with 15% wt ECZ (which from now on will be referred to as PVK:ECZ:C_{60}:EPNA). In order to check if aggregation of EPNA takes place in this composite, we have prepared a sample containing six times less EPNA, but the same amount of PVK. The electro-optic coefficient of this sample was found to be approximately six times smaller, indicating that no significant aggregation of EPNA takes place.

4.2. Properties of the photorefractive grating

Investigation with the two-beam coupling technique has shown the dominance of a phase-shifted refractive index grating in PVK:ECZ:C_{60}:EPNA. In figure 7, a 2BC trace (curve 1) reveals a value for φ that is around 25°. A similar low value of the phase shift was measured in another PVK-based composite and it was attributed to the coexistence of a local grating that was evolving next to the photorefractive one (but with a different time constant) [11]. This is clearly not the case, however, in PVK:ECZ:C_{60}:EPNA. Curve 2 in figure 7 is a 2BC trace measured at the very early stages of grating growth. The fact that the phase shift is similar to that in the steady state, leads to the conclusion that only one grating exists inside the sample.

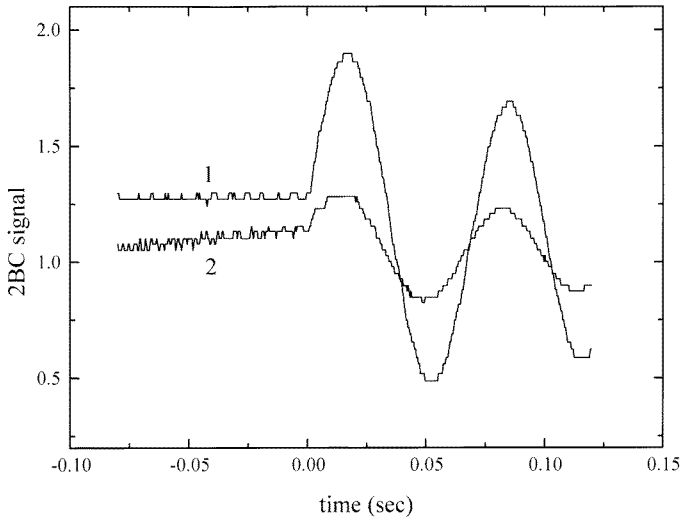

Figure 7. Two beam coupling traces in PVK:ECZ:C_{60}:EPNA at 55 V μm^{-1}. Trace 1: steady state regime. Trace 2: during the early stages of grating formation.

A small value of the phase shift indicates that the external electric field (or its projection along the grating wave vector in the tilted geometry used here), is smaller than or comparable to the saturation field [22]. The dependence of the gain coefficient and the diffraction

efficiency on the applied field, corroborates this hypothesis: the space charge field in this regime increases with the external field, which should, according to (4) and (5), cause a superlinear increase of Γ and $\eta^{0.5}$. This is shown in figure 8, where the curves are fits to power laws with exponents equal to 1.9 ± 0.2 and 1.5 ± 0.5, respectively. A Γ of 80 cm^{-1} is measured at 85 V μm^{-1}, that corresponds to a high net gain, as the absorption coefficient is less than 10 cm^{-1}. The value of the diffraction efficiency at this electric field is 20%.

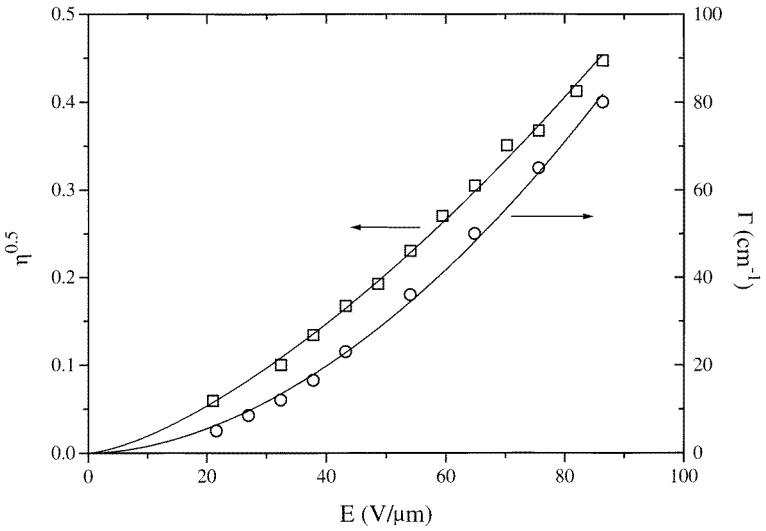

Figure 8. Electric field dependence of the gain coefficient and the square root of the diffraction efficiency for PVK:ECZ:C_{60}:EPNA. The curves are fits to a power law with exponents 1.5 ± 0.5 and 1.9 ± 0.2, respectively.

By decreasing the grating spacing to 0.2 μm (with the two beams incident at 45° from opposite faces, as in the inset of figure 9), thus decreasing the saturation field, the space charge field should lead to saturation. This is evident in figure 9, where the ratio of the square root of the diffraction efficiency to the applied field, that is directly proportional to E_{SC}, is plotted versus the applied field. A saturation is clearly observed above 50 V μm^{-1}.

The response time τ^{-1} of the photorefractive grating was measured with degenerate four-wave mixing. The decay of the diffraction efficiency under uniform illumination (500 mW cm^{-2}) was fitted to a squared exponential decay from which τ was derived. τ^{-1} was found to increase sublinearly with light intensity, obeying a power-law dependence with exponent equal to 0.65 ± 0.05. Similar behaviour has been observed in several other photorefractive polymers [9, 11, 30, 31] and is attributed to the presence of shallow traps.

The electric field dependence of τ^{-1} is shown in figure 10. The response time of the photorefractive grating in PVK-based polymers is believed to be limited by photogeneration [32]. This is reflected in the dependence of τ^{-1} on electric field, which is in agreement with the Onsager theory of geminate recombination [33]. Finally, the decay of the grating in the dark is shown in the inset of figure 10 to take place with two different time scales: a fast decay down to about 75% of the initial value is followed by a much slower one. The curve is a fit to a squared biexponential decay, revealing a dark storage time of around 16 min (slow component).

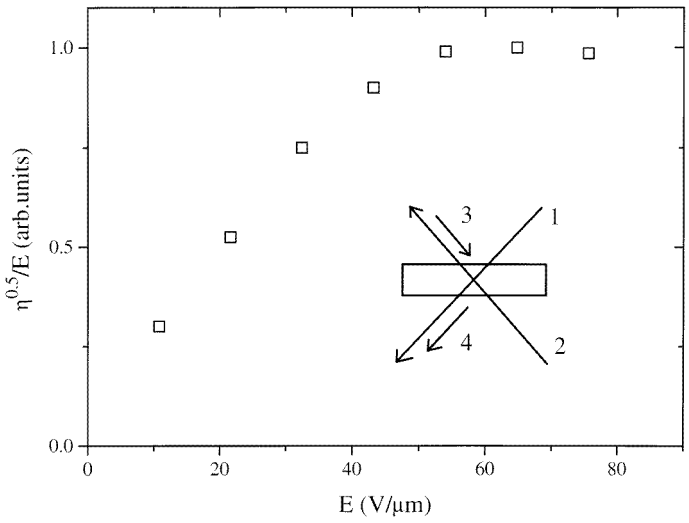

Figure 9. Electric field dependence of the ratio of the square root of the diffraction efficiency to the applied field for a grating spacing of 0.2 μm. Inset: the geometry of beam interaction with the two writing beams (1, 2), the reading beam (3) and the diffracted signal (4).

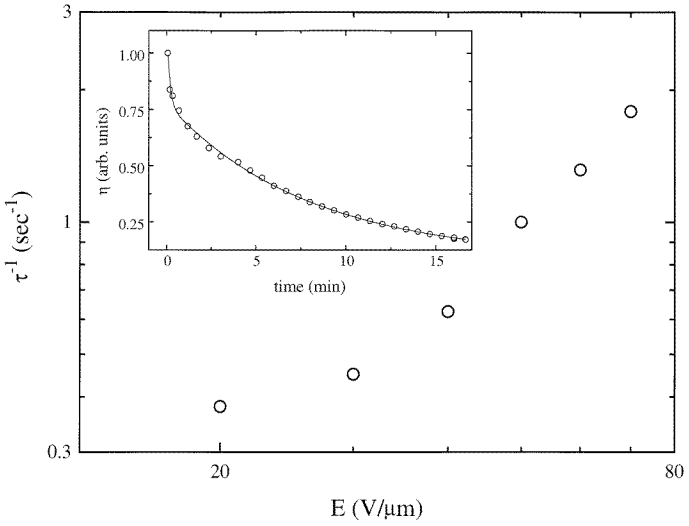

Figure 10. Electric field dependence of τ^{-1} under uniform illumination of 500 mW cm^{-2}. Inset: dark decay of the photorefractive grating at 55 V μm^{-1}. The curve is a fit to a squared biexponential decay, with time constants equal to 10 s and 16 min.

4.3. A configuration for high two-beam coupling gain and diffraction efficiency

The tilted geometry that is usually employed for the study of photorefractive polymers is not at the optimum. Due to Snell's law, the grating can only be formed with its wave vector tilted at a relatively large angle with respect to the applied field. This condition is relaxed using a configuration like the one in the inset of figure 11, where a prism is used to couple the beams inside the sample at a large angle. In this configuration, a higher projection of

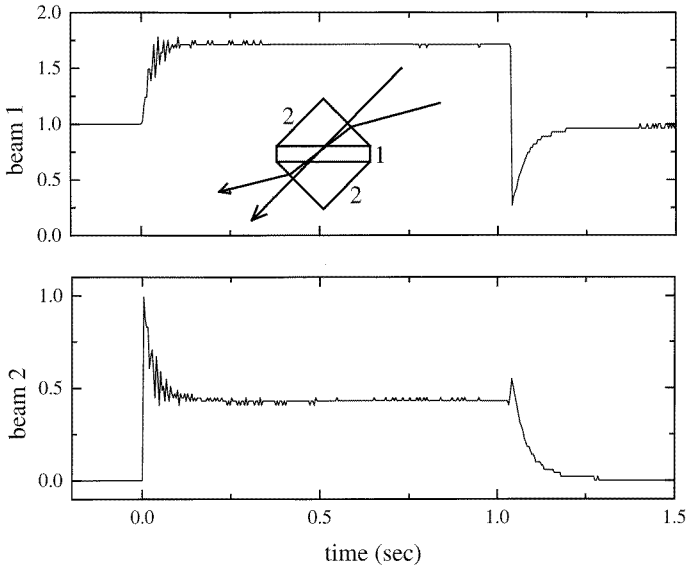

Figure 11. Energy exchange between two beams in the prism configuration. The electric field was 85 V μm^{-1}. Inset: the prism configuration with the sample (1) and the prisms (2). The two beams are incident at the prism at 0° and 30° with respect to the normal.

the electric field along the grating wave vector, a larger effective electro-optic coefficient and a longer interaction length of the two beams are achieved.

In figure 11, the energy exchange between two beams of approximately equal intensity is shown. As the second beam is switched on at time equal to zero, the photorefractive grating builds up, resulting in energy exchange between the two beams. The second beam is switched back off again after approximately 1 s and a strong depletion is evident in the first beam, as it is diffracted along the path of the second one. Finally, the diffracted beam decays as erasure of the grating takes place under the uniform illumination. The depletion of the first beam immediately after the second beam is switched off is almost 80%. Thus, with the simple addition of two prisms, an increase of about four times in the diffraction efficiency and of about two times in the two-beam coupling gain are achieved.

5. Conclusions

The mechanism of photorefractivity in a family of model composites based on PVK was examined. The refractive index change was shown to contain a contribution from the modulation of birefringence, arising from the reorientation of the NLO molecules in the space charge field. A modification of the trap density of the composites was demonstrated with the addition of a low ionization potential molecule. The influence of disorder on the space charge field formation process was observed. The effect of plasticization on the photorefractive properties was investigated.

Acknowledgments

Financial support from ‘Stichting Scheikundig Onderzoek Nederland’ (SON) and ‘Stichting Toegepaste Wetenschappen’ (STW) is gratefully acknowledged. GGM is grateful to Henk Angerman and Gerrit ten Brinke for fruitful discussions.

References

[1] Günter P and Huignard J P (eds) 1988 *Photorefractive Materials and Their Applications I, II* (Topics in Applied Physics **61**, **62**) (Berlin: Springer)
[2] Ducharme S, Scott J C, Twieg R J and Moerner W E 1991 *Phys. Rev. Lett.* **66** 1846
[3] Moerner W E, Silence S M, Hache F and Bjorklund G C 1994 *J. Opt. Soc. Am.* B **11** 320
[4] Borsenberger P M and Weiss D S (eds) 1993 *Organic Photoreceptors for Imaging Systems* (Optical Engineering **39**) (New York: Dekker)
[5] Prasad P N and Williams D J 1991 *Introduction to Nonlinear Optical Effects in Molecules and Polymers* (New York: Wiley)
[6] Bolink H J, Krasnikov V V, Malliaras G G and Hadziioannou G 1994 *Adv. Mater.* **6** 574
[7] Moerner W E and Silence S M 1994 *Chem. Rev.* **94** 127
[8] Donkers M C J M, Silence S M, Walsh C A, Hache F, Burland D M, Moerner W E and Twieg R J 1993 *Opt. Lett.* **18** 1044
[9] Orczyk M E, Swedek B, Zieba J and Prasad P N 1994 *J. Appl. Phys.* **76** 4995
[10] Meerholz K, Volodin B L, Sandalphon, Kippelen B and Peyghambarian N 1994 *Nature* **371** 497
[11] Poga C, Burland D M, Hanemann T, Jia Y, Moylan C R, Stankus J J, Twieg R J and Moerner W E 1995 *Xerographic Photoreceptors and Photorefractive Polymers* (*Proc. SPIE* **2526**) ed S Ducharme and P M Borsenberger
[12] Zobel O, Eckl M, Strohriegl P and Haarer D 1995 *Adv. Mater.* **7** 911
[13] Schildkraut J S 1990 *Appl. Opt.* **29** 2839
[14] Sutter K and Günter P 1990 *J. Opt. Soc. Am.* B **7** 2274
[15] Walsh C A and Moerner W E 1992 *J. Opt. Soc. Am.* B **9** 1642
[16] Malliaras G G 1995 *PhD Thesis* University of Groningen
[17] Kuzyk M G, Sohn J E and Dirk C W 1990 *J. Opt. Soc. Am.* B **7** 842
[18] Malliaras G G, Krasnikov V V, Bolink H J and Hadziioannou G 1994 *Appl. Phys. Lett.* **65** 262
[19] Orczyk M E, Zieba J and Prasad P N 1995 *Appl. Phys. Lett.* **67** 311
[20] Malliaras G G, Krasnikov V V, Bolink H J and Hadzioannou G 1995 *Appl. Phys. Lett.* **66** 1038
[21] Malliaras G G, Krasnikov V V, Bolink H J and Hadzioannou G 1995 *Appl. Phys. Lett.* **67** 455
[22] Kukhtarev N V, Markov V B, Odulov S G, Soskin M S and Vinetskii V L 1979 *Ferroelectrics* **22** 949, 961
[23] Bassler H 1993 *Phys. Stat. Sol.* b **175** 15
[24] Partanen J P, Jonathan J M C and Hellwarth R W 1990 *Appl. Phys. Lett.* **57** 2404
[25] Nouchi P, Partanen J P and Hellwarth M R W 1993 *Phys. Rev.* B **47** 15 581
[26] Jonathan J M C, Roussignol Ph and Roosen G 1988 *Opt. Lett.* **13** 224
[27] Malliaras G G, Krasnikov V V, Bolink H J and Hadziioannou G 1995 *Phys. Rev.* B **52** R14 324
[28] Malliaras G G, Angerman H, Krasnikov V V, ten Brinke G and Hadziioannou G 1996 *J. Phys. D: Appl. Phys.* submitted
[29] Scher H and Montroll E W 1975 *Phys. Rev*. B **12** 2455
[30] Silence S M, Walsh C A, Scott J C, Mattray T J, Twieg R J, Hache F, Bjorklund G C and Moerner W E 1992 *Opt. Lett.* **17** 1107
[31] Donkers M C J M, Silence S M, Walsh C A, Hache F, Burland D M, Moerner W E and Twieg R J 1993 *Opt. Lett.* **18** 1044
[32] Silence S M, Scott J C, Hache F, Ginsburg E J, Jenkner P K, Miller R D, Twieg R J and Moerner W E 1993 *J. Opt. Soc. Am.* B **12** 2306
[33] Onsager L 1938 *Phys. Rev.* **54** 554